MDPI

Dynamic Aether as a Trigger for Spontaneous Spinorization in Early Universe

Alexander Balakin *,† and Anna Efremova †

Department of General Relativity and Gravitation, Institute of Physics, Kazan Federal University, Kremlevskaya Str. 16a, Kazan 420008, Russia; anna.efremova131@yandex.ru

* Correspondence: alexander.balakin@kpfu.ru
† These authors contributed equally to this work.

Abstract: In the framework of the Einstein–Dirac-aether theory we consider a phenomenological model of the spontaneous growth of the fermion number, which is triggered by the dynamic aether. The trigger version of spinorization of the early Universe is associated with two mechanisms: the first one is the aetheric regulation of behavior of the spinor field; the second mechanism can be related to a self-similarity of internal interactions in the spinor field. The dynamic aether is designed to switch on and switch off the self-similar mechanism of the spinor field evolution; from the mathematical point of view, the key of such a guidance is made of the scalar of expansion of the aether flow, proportional to the Hubble function in the isotropic cosmological model. Two phenomenological parameters of the presented model are shown to be considered as factors predetermining the total number of fermions born in the early Universe.

Keywords: alternative theories of gravity; Einstein-aether theory; spinor

1. Introduction

The paper is written for the Special Issue of the journal Universe in Honor of Professor Richard Kerner on the Occasion of His 80th Birthday.

In 1996, Damour and Esposito-Farèse introduced the term "spontaneous scalarization" [1] in order to describe gravitational analogs of the phase transition of the second order in ferromagnetic materials. The phenomenological idea about spontaneous scalarization has been used in different astrophysical and cosmological contexts (see, e.g., [2–13]). This fruitful idea has been extended and applied to models in other fields, and now we can find works devoted to the problems of spontaneous vectorization (see, e.g., [14–16]), spontaneous tensorization [17], spontaneous spinorization [18,19], as well as to the problems of spontaneous polarization of the color aether [20,21] and of spontaneous growth of the gauge fields [22].

The formalism of the spontaneous growth of the mentioned physical fields is mainly connected with the mechanism of tachyonic instability. We consider the phenomenon of spontaneous spinorization but propose another mechanism based on the model of self-similarity of the internal interactions in the fermion systems. Below, we will discuss in detail this mechanism, but now we would like to focus on a new detail of our approach. We consider the spinor field in the framework of Einstein–Dirac-aether theory and assume that the unit time-like vector field U^j associated with the velocity four-vector of the dynamic aether is the key element of this theory. The theory of the dynamic aether (see, e.g., [23–28] for basic definitions and references) belongs to the category of vector-tensor modifications of gravity [29,30]. The presence of the unit vector field U^j in this theory realizes the idea of a preferred frame of reference (see, e.g., [31,32]) and indicates the possibility of violation of the Lorentz invariance [33,34].

Of course, it is hard to dispute the argument that the birth of particles is the field of quantum theory. However, the quantum version of the aetheric vector field is not

yet established, and there are no ideas as to what particles could be the carriers of the corresponding interactions. That is why we restrict ourselves by the phenomenological theory. In fact, we consider some macroscopic consequences of the interaction between the spinor and aether vector fields in order to formulate a hypothesis: when and how the spinorization provoked by the aether could happen in the early Universe.

What new detail does the involvement of the dynamic aether bring to the scheme of self-interaction of the spinor system? We assume that the aether regulates the dynamics of the fermion system. What is the instrument of the aetheric influence on the spinor field? We assume that the key instrument of such guidance is the expansion scalar $\Theta = \nabla_k U^k$. On the one hand, this true scalar is an intrinsic element of the aether flow. On the other hand, in the isotropic cosmological models of the Friedmann type $\Theta = 3H$, $H(t) = \frac{\dot{a}}{a}$ is the Hubble function. In other words, the scalar $\frac{3}{\Theta} = \frac{1}{H}$ defines the typical time scale, which characterizes the rate of the Universe evolution. Such a measure plays in the field theory the role analogous to the role of temperature when one describes the Universe evolution on the thermodynamic level. This analogy is consistent with the fact that both quantities, the effective temperature and the expansion scalar, are decreasing in the expanding Universe. However, when we consider analogies between the expansion scalar Θ in the field theory and the temperature T in the Universe thermodynamics, we can try to establish the analogy between the Curie temperature T_C in the theory of phase transitions of the second kind and some critical value Θ_*. Such an approach allows us to suppose the following: a new internal interaction in the fermion system is switching on, if $\Theta < \Theta_*$ just as when the phase transition in ferroelectrics takes place, if T becomes less than the Curie temperature $T < T_C$. To conclude, we suppose that the aetheric guidance is manifested in the fact that the aether is switching on (and switching off) the specific internal interaction in the fermion system in the manner of how the decreasing temperature switches on the reconstruction of ferromagnetic materials below the Curie temperature. Our purpose is to show that such a mechanism could explain the spontaneous growth of the spinor particle number in the early Universe.

The paper is organized as follows. In Section 2, we reconstruct the total Lagrangian of the model and derive the extended master equations for the unit vector, spinor, and gravitational fields. In Section 3, we consider the application to the isotropic cosmological model and derive the evolutionary equations for basic spinor invariants. In Section 4, we present the model function describing the self-similar interaction in the fermion system and analyze the solutions of the corresponding extended master equations. Section 5 includes discussion and conclusions.

2. The Formalism
2.1. Lagrangian of the Einstein–Dirac-Aether Theory

The canonic Lagrangian of the Einstein-aether theory

$$L_{(\text{EA})} = -\frac{1}{2\kappa}\left[R + 2\Lambda + \lambda(g_{mn}U^mU^n - 1) + K^{abmn}\nabla_a U_m \nabla_b U_n\right] \tag{1}$$

contains three principal parts [23]. In the first one, R is the Ricci scalar, Λ is the cosmological constant, and $\kappa = 8\pi G$ includes the Newtonian coupling constant G ($c = 1$). The second and third parts of the Lagrangian (1) contain the four-vector U^i, associated with the aether velocity. The term $\lambda(g_{mn}U^mU^n - 1)$ is designed to guarantee that the U^i is normalized to one; respectively, λ is the Lagrange multiplier. The so-called kinetic term $K^{abmn}\nabla_a U_m \nabla_b U_n$ is quadratic in the covariant derivative $\nabla_a U_m$ of the vector field U^i, with the tensor K^{abmn} to be constructed using the metric tensor g^{ij} and the aether velocity four-vector U^k only,

$$K^{abmn} = C_1 g^{ab}g^{mn} + C_2 g^{am}g^{bn} + C_3 g^{an}g^{bm} + C_4 U^a U^b g^{mn}. \tag{2}$$

The parameters C_1, C_2, C_3, and C_4 are the Jacobson coupling constants. The massive spinor field is described by the following term of the Lagrangian:

$$L_{(\mathrm{D})} = \frac{i}{2}[\bar{\psi}\gamma^k D_k\psi - D_k\bar{\psi}\gamma^k\psi] - m\bar{\psi}\psi \,. \tag{3}$$

Here, ψ defines the Dirac spinor field, $\bar{\psi}$ is the Dirac conjugated field, m is the mass prescribed to the spinor particle, γ^k are the Dirac matrices, and the covariant (extended) derivatives of the spinors

$$D_k\psi = \partial_k\psi - \Gamma_k\psi \,, \quad D_k\bar{\psi} = \partial_k\bar{\psi} + \bar{\psi}\Gamma_k \,, \tag{4}$$

are constructed using the Fock–Ivanenko connection matrices Γ_k [35].

If we intend to construct the action functional of a multi-component system, we have to obey the following rules. First, the SU(N) symmetric Yang–Mills fields and thus the U(1) symmetric Maxwell field add the contributions of the form $-\frac{1}{4}\mathbf{F}_{mn}\mathbf{F}^{mn}$ (see, e.g., [36]). Second, the scalar field introduces the term $\frac{1}{2}\left[\nabla_m\phi\nabla^m\phi - m^2\phi^2\right]$. Third, the spinor field adds the term (3) so that the Ricci scalar R, the invariant $\frac{1}{4}\mathbf{F}_{mn}\mathbf{F}^{mn}$, the Klein–Gordon mass term $m^2\phi^2$, and the spinor mass term $m\bar{\psi}\psi$ enter the action functional with the same sign minus. Taking into account this detail, we use in our work the following total action functional

$$-S_{(\mathrm{EDA})} = \int d^4x\sqrt{-g}\left\{\frac{1}{2\kappa}\left[R+2\Lambda+\lambda(g_{mn}U^mU^n-1)+K^{abmn}\nabla_aU_m\nabla_bU_n\right]+\right.$$

$$\left.+L_{(\mathrm{matter})} + \beta(\Theta, S, P^2) - \left[\frac{i}{2}[\bar{\psi}\gamma^k D_k\psi - D_k\bar{\psi}\gamma^k\psi] - m\bar{\psi}\psi\right]\right\}. \tag{5}$$

The term $L_{(\mathrm{matter})}$ describes the matter of non-spinor (non-fermionic) origin, e.g., the pseudo-Goldstone bosons attributed to the axionic dark matter. We include the minus sign into the left-hand side of this formula, keeping in mind that the variation procedure $\delta S_{(\mathrm{EDA})} = 0 = -\delta S_{(\mathrm{EDA})}$ gives the same master equations. In addition, we include into (5) the cross term $\beta(\Theta, S, P^2)$; the arguments of this function are described below.

2.2. Basic Assumptions and Auxiliary Definitions
2.2.1. Fock–Ivanenko Connection, Tetrad Four-Vectors, Spinor Scalar S, and Pseudoscalar P

The Fock–Ivanenko matrices

$$\Gamma_k = \frac{1}{4}g_{mn}X_s^{(a)}\gamma^s\gamma^n\nabla_k X_{(a)}^m \tag{6}$$

contain four tetrad four-vectors $X_{(a)}^m$, which satisfy the relationships

$$g_{mn}X_{(a)}^m X_{(b)}^n = \eta_{(a)(b)} \,, \quad \eta^{(a)(b)}X_{(a)}^m X_{(b)}^n = g^{mn} \,, \tag{7}$$

with the Minkowski metric $\eta_{(a)(b)}$. The convolutions $\gamma^k = X_{(a)}^k\gamma^{(a)}$ link the Dirac matrices γ^k depending on coordinates with the constant Dirac matrices $\gamma^{(a)}$. As usual, the Dirac matrices satisfy the fundamental anti-commutation relations

$$\gamma^{(a)}\gamma^{(b)}+\gamma^{(b)}\gamma^{(a)} = 2E\eta^{(a)(b)} \,, \quad \gamma^m\gamma^n+\gamma^n\gamma^m = 2Eg^{mn} \,, \tag{8}$$

where E is the unit matrix. In addition, we keep in mind the formula

$$\epsilon_{mnpq}X_{(a)}^m X_{(b)}^n X_{(c)}^p X_{(d)}^q = \epsilon_{(a)(b)(c)(d)} \,, \tag{9}$$

where ϵ_{mnpq} is the Levi-Civita tensor expressed via the absolutely antisymmetric symbol E_{mnpq} as follows:

$$\epsilon_{mnpq} = \sqrt{-g}E_{mnpq}\,, \quad E_{0123} = -1\,. \tag{10}$$

In the Minkowski spacetime $\sqrt{-g} = 1$, thus, $\epsilon_{(a)(b)(c)(d)} \equiv E_{(a)(b)(c)(d)}$ with $E_{(0)(1)(2)(3)} = -1$. Using (9), we can introduce in the covariant way the link between the Dirac matrices γ^5 and $\gamma^{(5)}$. Indeed, according to the basic definition

$$\gamma^5 = -\frac{1}{4!}\epsilon_{mnpq}\gamma^m\gamma^n\gamma^p\gamma^q\,, \tag{11}$$

we obtain

$$\gamma^5 = -\frac{1}{4!}\epsilon_{mnpq}X^m_{(a)}X^n_{(b)}X^p_{(c)}X^q_{(d)}\gamma^{(a)}\gamma^{(b)}\gamma^{(c)}\gamma^{(d)} =$$

$$=-\frac{1}{4!}\epsilon_{(a)(b)(c)(d)}\gamma^{(a)}\gamma^{(b)}\gamma^{(c)}\gamma^{(d)}=\gamma^{(0)}\gamma^{(1)}\gamma^{(2)}\gamma^{(3)} \equiv \gamma^{(5)}\,. \tag{12}$$

In other words, the matrix γ^5 defined by (11) does not depend on metric and, in addition to the unit matrix E, is a constant matrix. This fact allows us to introduce the scalar $S \equiv \bar{\psi}\psi = \bar{\psi}E\psi$ and the pseudoscalar $P \equiv i\bar{\psi}\gamma^5\psi = i\bar{\psi}\gamma^{(5)}\psi$. The scalar S is usually associated with the density of the spinor particle number. As for the definition of P, the multiplier i in front allows the matrix $i\gamma^5$ to be free of the imaginary unit.

2.2.2. Decomposition of the Covariant Derivative of the Aether Velocity Four-Vector

The tensor $\nabla_i U_k$ has the following standard decomposition into irreducible parts

$$\nabla_i U_k = U_i \mathcal{D}U_k + \sigma_{ik} + \omega_{ik} + \frac{1}{3}\Delta_{ik}\Theta\,. \tag{13}$$

Here, $\mathcal{D}U^i$ is the acceleration four-vector, σ_{ik} is the shear tensor, ω_{ik} is the vorticity tensor, Θ is the expansion scalar, Δ is the projector, and $\mathcal{D}$ is the convective derivative:

$$\mathcal{D}U_k \equiv U^m\nabla_m U_k\,, \quad \sigma_{ik} \equiv \frac{1}{2}\left(\overset{\perp}{\nabla}_i U_k + \overset{\perp}{\nabla}_k U_i\right) - \frac{1}{3}\Delta_{ik}\Theta\,, \quad \omega_{ik} \equiv \frac{1}{2}\left(\overset{\perp}{\nabla}_i U_k - \overset{\perp}{\nabla}_k U_i\right),$$

$$\Theta \equiv \nabla_m U^m\,, \quad \mathcal{D} \equiv U^i\nabla_i\,, \quad \Delta^i_k = \delta^i_k - U^i U_k\,, \quad \overset{\perp}{\nabla}_i \equiv \Delta^k_i\nabla_k\,. \tag{14}$$

Using the presented decomposition, one can say that there is one fundamental scalar Θ linear in the derivative and three additional quadratic scalars associated with the aether flow:

$$a^2 \equiv \mathcal{D}U_k\mathcal{D}U^k\,, \quad \sigma^2 \equiv \sigma_{ik}\sigma^{ik}\,, \quad \omega^2 \equiv \omega_{ik}\omega^{ik}\,. \tag{15}$$

In the model studied below, we use the new function $\beta(\Theta, S, P^2)$ of three arguments only; however, we hope to extend this modeling in the next works.

2.3. Master Equations

The variation procedure with respect to the Lagrange multiplier λ, aether velocity four-vector U^i, spinor field ψ, and its Dirac conjugate quantity $\bar{\psi}$, and with respect to the metric g^{pq} gives us the coupled system of master equations of the model. We start with the derivation of the aether dynamic equations.

2.3.1. Master Equations for the Aether Velocity

Variation of the total action functional (5) with respect to the Lagrange multiplier λ gives the condition $g_{ik}U^iU^k = 1$. Variation with respect to U^j yields

$$\nabla_a J^{aj} = I^j + \lambda U^j - \kappa \nabla^j \left(\frac{\partial \beta}{\partial \Theta} \right), \tag{16}$$

where the terms $\mathcal{J}^{aj}$ and I^j are defined as follows:

$$\mathcal{J}^{aj} = K^{abjn}(\nabla_b U_n), \quad I^j = C_4(\mathcal{D}U_m)(\nabla^j U^m), \tag{17}$$

and the Lagrange multiplier can be obtained as

$$\lambda = U_j\left[\nabla_a J^{aj} - I^j\right] + \kappa D\left(\frac{\partial \beta}{\partial \Theta}\right). \tag{18}$$

2.3.2. Master Equations for the Spinor Field

Variation with respect to $\bar{\psi}$ and ψ gives, correspondingly

$$i\gamma^n D_n \psi = M\psi, \quad iD_n\bar{\psi}\gamma^n = -\bar{\psi}M, \tag{19}$$

$$M \equiv \left(m + \frac{\partial \beta}{\partial S} \right) E + \frac{\partial \beta}{\partial P} i\gamma^5. \tag{20}$$

Based on the matrix M, we can introduce the effective mass of the interacting spinor field

$$< M > \equiv \frac{\bar{\psi}M\psi}{\bar{\psi}\psi} = \left(m + \frac{\partial \beta}{\partial S} \right) + \left(\frac{P}{S} \right) \frac{\partial \beta}{\partial P}. \tag{21}$$

2.3.3. Master Equations for the Gravity Field

Variation with respect to metric yields

$$R_{pq} - \frac{1}{2}g_{pq}R = \Lambda g_{pq} + T_{pq}^{(U)} + \kappa\left[T_{pq}^{(D)} + T_{pq}^{(M)} + T_{pq}^{(C)}\right], \tag{22}$$

where the following terms reconstruct the total stress–energy tensor

$$T_{pq}^{(U)} = \frac{1}{2}g_{pq}\,K^{abmn}\nabla_a U_m \nabla_b U_n + \lambda U_p U_q +$$

$$+C_1\left[(\nabla_m U_p)(\nabla^m U_q) - (\nabla_p U_m)(\nabla_q U^m)\right] + C_4\mathcal{D}U_p\mathcal{D}U_q +$$

$$+\nabla^m\left[U_{(p}\mathcal{J}_{q)m} - \mathcal{J}_{m(p}U_{q)} - \mathcal{J}_{(pq)}U_m\right], \tag{23}$$

$$T_{pq}^{(D)} = -g_{pq}L_D + \frac{i}{4}\left[\bar{\psi}\gamma_p D_q\psi + \bar{\psi}\gamma_q D_p\psi - (D_p\bar{\psi})\gamma_q\psi - (D_p\bar{\psi})\gamma_q\psi\right]. \tag{24}$$

The contribution of the non-spinor matter $T_{pq}^{(M)}$ is described by the standard formula

$$T_{pq}^{(M)} = -\frac{2}{\sqrt{-g}}\frac{\delta}{\delta g^{pq}}\left[\sqrt{-g}L_{(\text{matter})}\right]. \tag{25}$$

The cross-term $T_{pq}^{(C)}$ associated with the function $\beta(\Theta, S, P^2)$ is of the form

$$T_{pq}^{(C)} = g_{pq}\left[\beta - (D + \Theta)\frac{\partial \beta}{\partial \Theta}\right]. \tag{26}$$

Using the Dirac Equations (19), one can obtain that

$$L_D = [\bar{\psi}(M - mE)\psi] = \left[S \frac{\partial \beta}{\partial S} + P \frac{\partial \beta}{\partial P} \right]. \tag{27}$$

We used the following auxiliary formulas for the variation of tetrad four-vectors with respect to metric:

$$\delta X^j_{(a)} = \frac{1}{4} \left[X_{p(a)} \delta^j_q + X_{q(a)} \delta^j_p \right] \delta g^{pq}, \tag{28}$$

(see, e.g., [37] for details). In addition, we used the rules

$$\delta U^j = 0, \quad \delta \gamma^{(5)} = 0 = \delta \gamma^5, \quad \delta \gamma^{(a)} = 0, \quad \delta \gamma^k = \gamma^{(a)} \delta X^k_{(a)}. \tag{29}$$

3. Cosmological Application
3.1. Geometrical Aspects of the Model

For investigation of the spinorization phenomenon, we consider the spatially isotropic homogeneous spacetime platform with the FLRW type metric

$$ds^2 = dt^2 - a^2(t)[dx^{1^2} + dx^{2^2} + dx^{3^2}] \tag{30}$$

with the scale factor $a(t)$. For such a symmetry, the aether velocity four-vector has to be of the form $U^j = \delta^j_0$, and the covariant derivative is simplified essentially:

$$\nabla_k U^m = H(t) \left(\delta^m_1 \delta^1_k + \delta^m_2 \delta^2_k + \delta^m_3 \delta^3_k \right), \tag{31}$$

where $H(t) \equiv \frac{\dot{a}}{a}$ is the Hubble function (here and below the dot symbolizes the derivative with respect to time). The corresponding acceleration four-vector, shear tensor, and vorticity tensor vanish, and the expansion scalar $\Theta = \nabla_k U^k$ is equal to $\Theta = 3H$.

The sum of the Jacobson coupling constants $C_1 + C_3$ has been estimated in 2017 as the result of observation of the binary neutron star merger (the events GW170817 and GRB 170817A [38]). It was established that the ratio of the velocities of the gravitational and electromagnetic waves satisfies the inequalities $1 - 3 \times 10^{-15} < \frac{v_{gw}}{c} < 1 + 7 \times 10^{-16}$). According to [24], the square of the velocity of the tensorial aether mode is equal to $S^2_{(2)} = \frac{1}{1-(C_1+C_3)}$, thus, the sum of the parameters $C_1 + C_3$ can be estimated as $-6 \times 10^{-15} < C_1 + C_3 < 1.4 \times 10^{-15}$. Clearly, we can consider that with very high precision, $C_3 = -C_1$. The parameter C_4 does not enter the key formulas since $DU^j = 0$ for the FLRW model. As for the parameters C_1 and C_2, the results of the discussion about their constraints [39–42]) allows us to use the estimation $-\frac{2}{27} < C_2 < \frac{2}{21}$ (see [43]).

Taking into account these details, as well as the facts that for the isotropic homogeneous model, the acceleration four-vector and the shear and voricity tensors vanish, i.e., $DU^j = 0$, $\sigma_{mn} = 0$, and $\omega_{mn} = 0$, we see that the tensor J^{aj} is symmetric, and its nonzero components are the following:

$$J^a_j = (C_1 + C_4)U^a DU_j + C_3 U_j DU^a + (C_1 + C_3)\sigma^a_j + (C_1 - C_3)\omega^a_j C_3) + \frac{1}{3}(C_1 + C_3)\Delta^q_j \Theta + C_2 \Theta \delta^a_j =$$

$$= C_2 \Theta \delta^a_j. \tag{32}$$

The equations for the unit vector field (16) convert now into one equation

$$C_2 D\Theta + \kappa D \left(\frac{\partial \beta}{\partial \Theta} \right) = \lambda, \tag{33}$$

which gives, in fact, the solution for the Lagrange multiplier λ.

Our supplementary assumption is that the non-spinor matter is a cold dust and its stress–energy tensor is divergence-free, $\nabla^q T_{pq}^{(M)} = 0$, providing that $T_{pq}^{(M)} = \rho U_p U_q$ (ρ is the corresponding energy density scalar). Then, the equations for the gravitational field can be reduced to the following one equation

$$\frac{1}{\kappa}\left[3H^2\Gamma - \Lambda\right] = (\rho + mS) + \beta - \Theta\frac{\partial\beta}{\partial\Theta}\,. \tag{34}$$

Here, we introduce a new auxiliary parameter:

$$\Gamma = 1 + \frac{3}{2}C_2\,. \tag{35}$$

Other Einstein's equations are the differential consequences of the evolutionary equations for the aether and spinor fields. As a consequence of the separate conservation law for the non-fermionic matter, we obtain the standard law of its evolution

$$\dot{\rho} + 3H\rho = 0 \;\Rightarrow\; \rho(t) = \rho(t_0)\frac{a^3(t_0)}{a^3(t)}\,. \tag{36}$$

For the metric (30), the set of the tetrad four-vectors is

$$X_{(0)}^i = U^i = \delta_0^i\,, \quad X_{(\alpha)}^i = \delta_\alpha^i\frac{1}{a(t)}\,, \quad (\alpha = 1, 2, 3)\,, \tag{37}$$

and the spinor connection coefficients (6) have the form

$$\Gamma_0 = 0\,, \quad \Gamma_\alpha = \frac{1}{2}\dot{a}\gamma^{(\alpha)}\gamma^{(0)}\,. \tag{38}$$

We also use the direct consequence of (38)

$$\gamma^k\Gamma_k = -\frac{3}{2}H\gamma^0 = -\Gamma_k\gamma^k\,. \tag{39}$$

3.2. Reduced Evolutionary Equation for the Spinor Field

We assume that the components of the spinor field are the functions of the cosmological time only; then, the Dirac Equations (19) yield

$$i\gamma^0\left(\partial_0 + \frac{3}{2}H\right)\psi = M\psi\,, \tag{40}$$

$$i\left(\partial_0 + \frac{3}{2}H\right)\bar{\psi}\gamma^0 = -\bar{\psi}M\,. \tag{41}$$

If one uses the replacement

$$\psi = a^{-\frac{3}{2}}\Psi\,, \quad \bar{\psi} = a^{-\frac{3}{2}}\bar{\Psi}\,, \tag{42}$$

the Dirac equations take the form

$$i\gamma^{(0)}\dot{\Psi} = M\Psi\,, \quad i\dot{\bar{\Psi}}\gamma^{(0)} = -\bar{\Psi}M\,. \tag{43}$$

3.3. Evolution of the Spinor Invariants

Keeping in mind Equations (43), we can find the rates of evolution of the invariants S and P. First, we see that

$$\frac{d}{dt}(\bar{\psi}\psi) = \frac{d}{dt}\left(\bar{\Psi}a^{-3}\Psi\right) = -3H(\bar{\psi}\psi) + a^{-3}\left[\left(\frac{d}{dt}\bar{\Psi}\right)\gamma^{(0)^2}\Psi + \bar{\Psi}\gamma^{(0)^2}\left(\frac{d}{dt}\Psi\right)\right] =$$

$$= -3H(\bar{\psi}\psi) + i\bar{\psi}\left(M\gamma^0 - \gamma^0 M\right)\psi. \tag{44}$$

Using (20), we can present the evolutionary equation for the scalar S as follows:

$$\dot{S} + 3HS = -2T\frac{\partial\beta}{\partial P}. \tag{45}$$

The evolutionary equation for the pseudoinvariant P is

$$\dot{P} + 3HP = -\bar{\psi}\left(M\gamma^0\gamma^5 - \gamma^5\gamma^0 M\right)\psi, \tag{46}$$

$$\dot{P} + 3HP = 2T\left(\frac{\partial\beta}{\partial S} + m\right), \tag{47}$$

where the following auxiliary function T is introduced:

$$T \equiv \bar{\psi}\gamma^5\gamma^0\psi. \tag{48}$$

The auxiliary function $T(t)$ itself satisfies the equation

$$\dot{T} + 3HT = -i\bar{\psi}\left(M\gamma^5 + \gamma^5 M\right)\psi, \tag{49}$$

or equivalently

$$\dot{T} + 3HT = -2P\left(m + \frac{\partial\beta}{\partial S}\right) - 2S\frac{\partial\beta}{\partial P}. \tag{50}$$

In other words, the set of functions $S(t)$, $P(t)$, and $T(t)$ forms the closed evolutionary system.

One can explicitly check that the set of Equations (45), (47), and (50) for arbitrary β admits the so-called first integral. Indeed, the direct differentiation gives

$$\frac{d}{dt}\left(S^2 - P^2 - T^2\right) + 6H\left(S^2 - P^2 - T^2\right) = 0, \tag{51}$$

providing that

$$S^2 - P^2 - T^2 = \frac{\text{const}}{a^6}. \tag{52}$$

For further progress, it is convenient to introduce the variable $x = \frac{a(t)}{a(t_0)}$, the dimensionless scale factor, where t_0 is some fixed moment of the cosmological time. In addition, we introduce three auxiliary functions of this variable:

$$X = x^3 S, \quad Y = x^3 P, \quad Z = x^3 T, \tag{53}$$

so that the first integral (52) takes the form

$$X^2 - Y^2 - Z^2 = K \tag{54}$$

with arbitrary constant of integration K. In these terms, the evolutionary equations for $X(x)$ and $Y(x)$ take, respectively, the forms:

$$X'(x) = -\frac{6}{x\Theta} Z \left[\frac{\partial \beta}{\partial P} \right], \tag{55}$$

$$Y'(x) = \frac{6}{x\Theta} Z \left[m + \frac{\partial \beta}{\partial S} \right], \tag{56}$$

where Z has to be extracted from (54), i.e.,

$$Z = \pm \sqrt{X^2 - Y^2 - K} \tag{57}$$

with positive, negative, or vanishing parameter K.

1. When K is positive, i.e., $K = \nu^2 > 0$, the parametrization of the relationship (54) is

$$X = \nu \cosh u(x), \quad Y = \nu \sinh u(x) \cos v(x), \quad Z = \nu \sinh u(x) \sin v(x), \tag{58}$$

where $u(x)$ and $v(x)$ are real functions.

2. When K is negative, i.e., $K = -\mu^2 < 0$, we have the following parametrization of (54):

$$X = \mu \sinh u(x), \quad Y = \mu \cosh u(x) \cos u(x), \quad Z = \mu \cosh u(x) \sin v(x). \tag{59}$$

3. When $K = 0$, we deal with the parametrization

$$X = u(x), \ Y = u(x) \cos v(x), \ Z = u(x) \sin v(x). \tag{60}$$

In the first and second cases, we deal with the hyperbolic laws of evolution of the function X describing the number density of spinor particles.

4. Modeling of the Interaction Term

We would like to mention that new contributions to the Lagrangian, which have the form $F(S, P^2)$, were already considered in the nonlinear versions of the Einstein–Dirac models (see, e.g., [44–47]). In addition, the models describing the interaction of the spinor and scalar fields [48], as well as the spinor and pseudoscalar (axion) fields, ref. [49] have been studied. We introduce the new element of the Lagrangian $\beta(\Theta, S, P^2)$, which depends on the scalar of expansion of the aether flow $\Theta = \nabla_k U^k$. Our ansatz is that the scalar β as a function of the expansion scalar Θ is step-like:

$$\beta(\Theta, S, P^2) = \eta(\Theta_* - \Theta) \, \eta(\Theta - \Theta_{**}) B(S, P^2), \tag{61}$$

where $\eta(\mathcal{F})$ is the Heaviside function, which is equal to zero if $\mathcal{F} < 0$ and is equal to one if $\mathcal{F} > 0$. This means that there exists some moment of the cosmological time t_* when the interaction, described by the function β, switches on. At this moment, we fix the dimensionless scale factor $x(t_*) \equiv x_*$ and the corresponding values $\Theta_* \equiv \Theta(t_*)$ and $H_* \equiv H(t_*)$. Similarly, we introduce the time moment t_{**} when this interaction switches out. In other words, the aether flow guides the evolution of the spinor field. From the mathematical point of view, one has to solve the set of evolutionary equations in three domains: first, when $t_0 < t < t_*$; second, when $t_* < t < t_{**}$; third, when $t > t_{**}$. We assume that namely the second time interval relates to the spinorization phenomenon. At the borders $t = t_*$ and $t = t_{**}$, the functions $B(t)$, $S(t)$, $P(t)$, and $H(t)$ are assumed to be continuous. We use in our assumptions the analogy with ferroelectric materials, which possess a pair of Curie temperatures T_{C1} and T_{C2}. Let us start the analysis for the first indicated interval.

4.1. Solutions for the First Interval

Let us consider the first interval of the cosmological time $t_0 < t < t_*$ ($1 < x < x_*$). When $\beta = 0$, we see from (55) that

$$X' = 0 \Rightarrow S(x) = \frac{S(1)}{x^3}, \tag{62}$$

where $S(1) \equiv S(x(t_0))$ is the starting density of a number of the spinor particles. Keeping in mind (36), we find from Equation (34) the following Hubble function (in terms of x):

$$H(x) = \pm\sqrt{\frac{\Lambda}{3\Gamma}}\sqrt{1 + \frac{\kappa}{\Lambda x^3}[\rho(1) + mS(1)]}. \tag{63}$$

For the description of the expanding Universe, we have to choose the sign plus in (63) and obtain that the function $H(x)$ is monotonic and is falling, i.e., $H'(x) < 0$. The prime symbolizes the derivative with respect to x. We see that $H_* < H(1)$ and thus $\Theta_* < \Theta(1)$. Keeping in mind the relationship

$$t - t_0 = \int_1^{\frac{a(t)}{a(t_0)}} \frac{dx}{xH(x)}, \tag{64}$$

we obtain the following result of integration:

$$\frac{a(t)}{a(t_0)} = \left\{\cosh\left[\sqrt{\frac{3\Lambda}{4\Gamma}}(t-t_0)\right] + \sqrt{1 + \frac{\kappa}{\Lambda}[\rho(t_0) + mS(t_0)]}\,\sinh\left[\sqrt{\frac{3\Lambda}{4\Gamma}}(t-t_0)\right]\right\}^{\frac{2}{3}}. \tag{65}$$

Respectively, the effective mass coincides with the standard one, $< M >= m$.

4.2. Solutions for the Second Interval

We consider now the second interval of the cosmological time $t_* < t < t_{**}$ ($x_* < x < x_{**}$).

4.2.1. Hypothesis of Self-Similarity

In order to clarify the choice of the function $B(S, P^2)$, one can mention that the scalar $\bar{\psi}\psi$ plays the role of the fermion number when we consider a fermion as a realization of the Dirac field. The quantities $P = i\bar{\psi}\gamma^5\psi$ and $S = \bar{\psi}\psi$ themselves depend on the number of fermions in the Dirac system, however, their scalar ratio $\frac{P^2}{S^2}$ does not. Situations in physics, when the typical behavior of the dense system is similar to the one of the dilute system, are characterized by the specific term self-similarity. Below, we assume that the function $B(S, P^2)$ has just a self-similar form

$$B(S, P^2) = SF(Q), \quad Q = \frac{P^2}{S^2}, \tag{66}$$

and obtain that the effective mass (21) takes the form

$$< M >= m + F(Q). \tag{67}$$

Combining Equations (55) and (56), we obtain

$$\frac{dY}{dX} = \frac{Y}{X} - \frac{X}{Y}\left[\frac{m + F(Q)}{2F'(Q)}\right], \tag{68}$$

or equivalently

$$X\frac{dQ}{dX} = -\left[\frac{m + F(Q)}{2F'(Q)}\right]. \tag{69}$$

The solution to this equation is

$$F(Q) = -m + \frac{\text{const}}{X}, \tag{70}$$

providing that

$$B(S, P^2) = SF(Q) = -mS(x) + \frac{\text{const}}{x^3}. \tag{71}$$

We can find the constant of integration in (71) using the continuity requirements

$$B(x_*) = 0, \quad \lim_{x \to x_* - 0} S(x) = \lim_{x \to x_* + 0} S(x). \tag{72}$$

Clearly, we obtain

$$\text{const} = mx_*^3 S(x^*) = mS(1). \tag{73}$$

This means that the right-hand side of the gravity field in Equation (34)

$$\rho + mS + SF(Q) - \Theta\delta(\Theta - \Theta_*)SF(Q) = \frac{\rho(1)}{x^3} + \frac{mS(1)}{x^3} \tag{74}$$

keeps the same form as at $t_0 < t < t_*$. In other words, the solution for the scale factor coincides by the form with (65), but we have to replace t_0 with t_*, describing the starting point of the arguments of hyperbolic functions in the second time interval.

The function $Y^2(x)$ can be now presented as

$$Y^2 = X^2 F^{-1}\left[-m + \frac{mS(1)}{X}\right] \tag{75}$$

in terms of the inverse function F^{-1}. Thus, we need to solve Equation (55) and extract the fermion density number function $S(x) = \frac{X(x)}{x^3}$. This task can be solved only numerically, which is why to have some analytical progress, we consider below the linear function $F(Q) \to -m_* + h_0 Q$.

Remark. *At the end of this paragraph, it is convenient to make the remark concerning the formal discontinuity, which appears due to the presence of the delta function $\delta(\Theta_* - \Theta)$, the derivative of the Heaviside function $\eta(\Theta_* - \Theta)$ (see (61)) with respect to its argument. Clearly, the Lagrange parameter λ (18), the term $\lambda U_p U_q$ in (23), and the term (26) contain this delta function. As the result, the right-hand side of the key gravity field equation (74) also includes the delta function. Why does this discontinuity disappear when we solve the key equations? According to the continuity requirement $B(x_*) = 0$ (see (72)), we obtain that $\Theta = \Theta_*$ just when $t = t_*$ and $x = x_*$, thus, the term $B(x)\delta(\Theta_* - \Theta)$ disappears at $t = t_*$. The situation with $t = t_{**}$ is similar.*

4.2.2. Linear Function Describing Self-Similarity

Let us consider the function $B(S, P^2)$ in the form

$$B(S, P^2) = -m_* S + h_0 \frac{P^2}{S}, \tag{76}$$

where m_* and h_0 are some phenomenological parameters. We obtain now

$$Q(X) = \xi + \frac{mS(1)}{h_0 X}, \tag{77}$$

where a new guiding parameter ξ appears

$$\xi = \left(\frac{m_* - m}{h_0}\right). \tag{78}$$

Now, Equation (55) can be rewritten as follows:

$$\frac{dX}{dx} = \mp \frac{4h_0\sqrt{Q}}{xH} \sqrt{X^2(1-Q)-K}.$$ (79)

Clearly, this equation admits separation of variables

$$\frac{\sqrt{X}dX}{\sqrt{\xi X + \frac{mS(1)}{h_0}}\sqrt{X\left[(1-\xi)X - \frac{mS(1)}{h_0}\right]-K}} = \mp 4h_0 dt,$$ (80)

but further analytic progress is possible for specific choice of the guiding parameters ξ and K. Below, we consider two special submodels: first, when $\xi = 0$ and $K = 0$; second, when $\xi = \frac{1}{2}$ and $K = 0$.

4.2.3. The First Special Submodel

When $K = 0$, we work with the function $Z = \pm\sqrt{X^2-Y^2}$, and when $\xi = 0$, we see that $m_* = m$. For this choice of the guiding parameters, we obtain the exactly integrable submodel with

$$X(t) = \frac{mS(1)}{h_0}\left[1 + 4h_0^2(t-t_+)^2\right],$$ (81)

$$Y(t) = \frac{mS(1)}{h_0}\sqrt{1 + 4h_0^2(t-t_+)^2}.$$ (82)

Here, we used the new auxiliary quantity

$$t_+ = t_* + \sqrt{\frac{h_0 - m}{4mh_0^2}}.$$ (83)

In addition, we used the boundary condition $X(t_*) = x_*^3 S(x_*) = S(1)$, we have chosen the upper sign in (80) so that $t_+ > t_*$, and we have assumed that $h_0 \geq m$.

The effective mass depends on time as follows:

$$< M >= h_0 Q(t) = \frac{h_0}{\left[1 + 4h_0^2(t-t_+)^2\right]}.$$ (84)

The function $< M > (t)$ starts with the value m at $t = t_*$ then reaches the maximal value $< M >_{(\max)} = h_0 \geq m$ at the moment $t = t_{\max} = t_+$, and then it decreases monotonically. The time moment $t_{\max} = t_+$ is the function of the parameter h_0 (see (83)); when $h_0 = m$, $t_{\max} = t_*$; when $m < h_0 < 2m$, this function grows and reaches the maximum at $h_0 = 2m$; when $h_0 > 2m$, the parameter $t_{\max}$ decreases and tends to t_*. In other words, when the guiding parameter h_0 monotonically grows, the maximum of the function $< M > (t)$ drifts to the late time moments then stops and starts to drift to the initial point t_*. Figure 1 illustrates the behavior of the reduced function $\frac{<M>}{m}$ for the cases when $h_0 \geq 2$.

The spinor particle number density is presented as

$$s(t) \equiv \frac{S(t)}{S(t_*)} = \frac{\left(\frac{m}{h_0}\right)\left[1 + 4h_0^2(t-t_+)^2\right]}{\cosh^2\left[\sqrt{\frac{3\Lambda}{4\Gamma}}(t-t_*)\right]\left\{1 + \sqrt{1 + \frac{\kappa}{\Lambda}(\rho(t_0)+mS(t_0))}\tanh\left[\sqrt{\frac{3\Lambda}{4\Gamma}}(t-t_*)\right]\right\}^2}.$$ (85)

This function depends on the parameters Λ, Γ, m, h_0, and on the initial values $\rho(t_0)$, $S(t_0)$, so that the behavior of this function is much more sophisticated than the behavior of $< M >$. However, the numerical analysis shows that the corresponding graphs possess maxima. If we fix Λ, Γ, m, $\rho(t_0)$, $S(t_0)$ and consider variation of the guiding parameter

h_0 only, we can state the following: first, the height of the maximum increases when the parameter h_0 grows; second, the maximum of the corresponding graph starts to shift to the late time moments, stops, and then moves towards lower values of time. Figure 2 illustrates the details of such behavior.
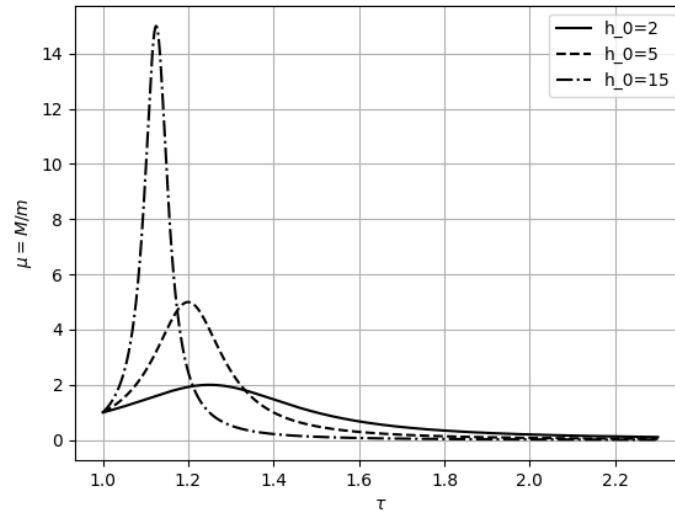

Figure 1. Illustration of the behavior of the ratio $\mu \equiv \frac{<M>}{m}$ for the model with $\xi = 0$ (see (84)) as the function of time and of the guiding parameter h_0. For illustration on all the figures, we set $m = 1$, $t_* = 1$ and measured the cosmological time in the dimensionless units $\tau = tH_0$ ($H_0 = \sqrt{\frac{\Lambda}{3}}$). The maximal values of all functions $\mu(t, h_0)$ are equal to h_0. For $h_0 > 2m$, the values of μ grow with h_0 and the maxima of the corresponding graphs shift to the initial moment t_*.
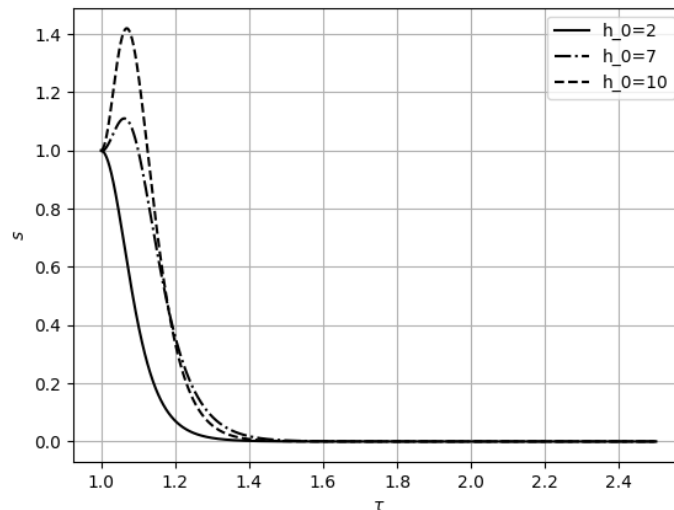

Figure 2. Illustration of the behavior of the dimensionless function $s(t) \equiv \frac{S(t)}{S(t_*)}$ for the model with $\xi = 0$ (see (85)) when the parameters Λ, Γ, m, $\rho(t_0)$, $S(t_0)$ are fixed and only the guiding parameter h_0 is varying.

4.2.4. The Second Special Submodel

The condition $\xi = \frac{1}{2}$ is equivalent to $m_* - m = \frac{1}{2}h_0$. The key Equation (80) for the function X reads now

$$\frac{dX}{\sqrt{\frac{1}{4}X^2 - \left(\frac{mS(1)}{h_0}\right)^2}} = \mp 4h_0 dt. \tag{86}$$

The solution, which corresponds to the upper sign in (86) and to the condition $h_0 > 2m$, is

$$\frac{X(t)}{X(t_*)} = \cosh 2h_0(t-t_*) - \sqrt{1 - \frac{4m^2}{h_0^2}} \sinh 2h_0(t-t_*), \tag{87}$$

or equivalently

$$s(t) = \frac{S(t)}{S(t_*)} = \frac{\cosh\left[2h_0(t-t_*)\right]\left\{1 - \sqrt{1 - \frac{4m^2}{h_0^2}} \tanh\left[2h_0(t-t_*)\right]\right\}}{\cosh^2\left[\sqrt{\frac{3\Lambda}{4\Gamma}}(t-t_*)\right]\left\{1 + \sqrt{1 + \frac{\kappa(\rho(t_0)+mS(t_0))}{\Lambda}} \tanh\left[\sqrt{\frac{3\Lambda}{4\Gamma}}(t-t_*)\right]\right\}^2}. \tag{88}$$

The effective mass evolves with respect to the law

$$<M> = \frac{m}{\cosh 2h_0(t-t_*) - \sqrt{1 - \frac{4m^2}{h_0^2}} \sinh 2h_0(t-t_*)}. \tag{89}$$

At $t = t_*$, we obtain $<M>(t_*) = m$. The function $<M>(t)$ reaches the maximal value $<M>_{(\max)} = \frac{h_0}{2}$, where $t_{\max}$ is defined as

$$\cosh\left[2h_0(t_{\max} - t_*)\right] = \frac{h_0}{2m}, \tag{90}$$

or equivalently

$$t_{\max} = t_* + \frac{1}{2h_0} \log\left[\frac{h_0}{2m}\left(1 + \sqrt{1 - \frac{4m^2}{h_0^2}}\right)\right]. \tag{91}$$

The quantity $t_{\max}$ as the function of the guiding parameter h_0 increases when the parameter h_0 grows, reaches the maximum, and then monotonically tends to t_*. In other words, when the guiding parameter h_0 monotonically grows, the maximum of the function $<M>(t)$ drifts to the late time moments, then stops and starts to drift to the initial point t_*, as in the submodel with $\xi = 0$. Figure 3 illustrates the behavior of the reduced function $\frac{<M>}{m}$ for the cases when this maximum is passed.
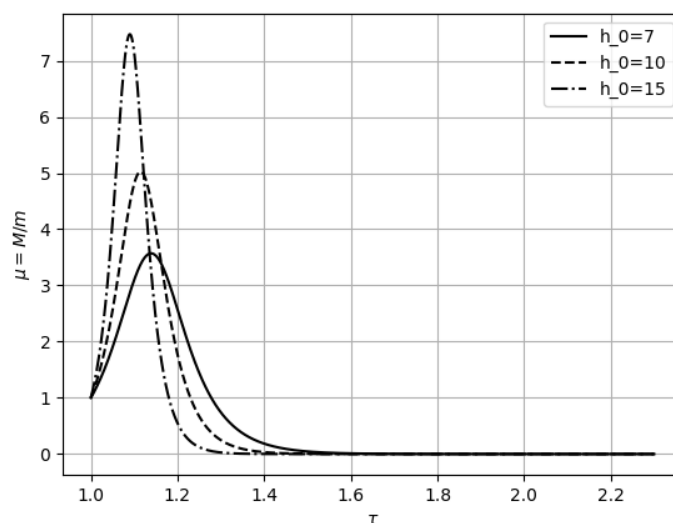

Figure 3. Illustration of the behavior of the ratio $\mu \equiv \frac{<M>}{m}$ for the model with $\xi = \frac{1}{2}$ (see (89)) as the function of time and of the guiding parameter h_0. The maximal values of all functions $\mu(t, h_0)$ are equal to $\frac{1}{2}h_0$. For $h_0 > 2m$, the values of μ grow with h_0 and the maxima of the corresponding graphs shift to the initial moment t_*.

The behavior of the function $s(t)$ (88) is similar to the one for the model with $\xi = 0$. Again, the graphs demonstrate the maxima, which move similarly. Figure 4 illustrates this behavior.
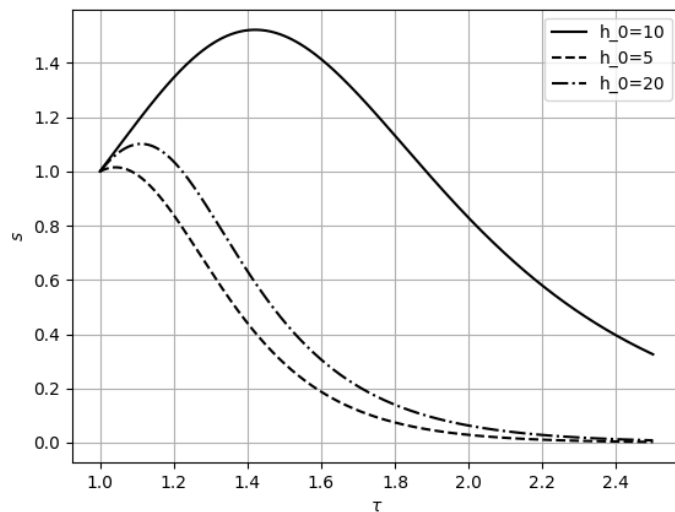

Figure 4. Illustration of the behavior of the dimensionless function $s(t) \equiv \frac{S(t)}{S(t_*)}$ for the model with $\xi = \frac{1}{2}$ (see (88)) when the parameters $\Lambda, \Gamma, m, \rho(t_0), S(t_0)$ are fixed and only the guiding parameter h_0 is varying. According to the legend, when h_0 grows, the maximum of the graph shifts to the late time moments then stops and starts to drift towards the initial time moment. The heights of the maxima of the graphs increase on the first stage and decrease on the second one.

4.3. On the Solutions for the Third Interval

During the third stage of the Universe evolution ($t > t_{**}$), we deal with $\beta = 0$, the value of the scalar S on the boundary $t = t_{**}$ is predetermined by the formulas already found for the interval $t_0 < t < t_*$. The process of spinorization is finished.

5. Discussion and Conclusions

5.1. The Role of Guiding Model Parameters

We presented an exactly integrable phenomenological model according to which the dynamic aether coupled to the spinor field opens a window for the spontaneous growth of the fermion number in the early Universe. We have to emphasize that this spontaneous growth is the result of internal self-interaction in the spinor system, which we indicated as a mechanism of self-similar coupling. As for the dynamic aether, it plays the role of regulator for this process. Our purpose was to show explicitly that the function $S(t) = \bar{\psi}\psi$, which is usually associated with the number density of the spinor particle, can grow, can reach some maximal value, and then can monotonically decrease under the influence of the Universe expansion. The formula (85) describes this statement for the first model with the guiding model parameter $\xi = 0$, and the formula (88) confirms this statement for the model with $\xi = \frac{1}{2}$. It is required to say a few words about the parameters of the whole model. First, we use the cosmological constant Λ; second, only one Jacobson coupling constant C_2 appears in the master equations reduced for the chosen spacetime symmetry. Final formulas contain the unified parameter $H_\infty = \sqrt{\frac{\Lambda}{3\left(1 + \frac{3}{2}C_2\right)}}$, which gives the asymptotic value of the Hubble function H_∞, different from the de Sitter parameter $H_0 = \sqrt{\frac{\Lambda}{3}}$. The model of self-similar interaction includes additional parameters ξ (78) and h_0. It turned out that the parameter h_0 predetermines the maximal value of the effective spinor mass $< M >$ (21). In addition, we introduced phenomenologically two time moments t_* and t_{**}, which restrict the interval inside of which the dynamic aether "allows" the spinor field to switch on the self-similar interaction; we consider the corresponding values of the

expansion scalar $\Theta_* \equiv \Theta(t_*)$ and $\Theta_{**} \equiv \Theta(t_{**})$ as the analogs of the first and second Curie temperatures in ferroelectrics. The last guiding parameter of the model is the so-called "seed mass" m. This value of the spinor mass is not fixed in the model. there are several ideas about this quantity. For instance, the collision of pairs of photons could produce the electron–positron pairs when the photon energy was sufficient to overcome the barrier of the electron rest energy $2m_e$. In this case, the electron mass m_e could be the seed mass $m \to m_e$. The corresponding initial fermion number density was indicated as $S(t_0)$.

5.2. The Role of the Effective Spinor Mass

In the thermodynamics of the hot Universe, there exists a hypothesis that when the thermal energy $k_B T$ is equal to the sum of the rest energies of pairs of particles, $k_B T = 2\mathcal{M}c^2$, these particles can emerge as the individual ones (particles drop out from the equilibrium fluid). We put forward a hypothesis that in analogy with the thermodynamic approach, the specific spinor particles can appear as the individual ones when their masses (predicted by the quantum theory) coincide with the effective mass $< M >$. Is it possible on the basis of our hypothesis to explain the birth of spinors of all known types?

In the standard units, we have to replace $m \to \frac{mc}{\hbar}$. For the special units with $c = 1$ and $\hbar = 1$, this mass parameter is presented as usual in MeV. From the standard catalog of fermion masses, we know the following: first, the masses of the quarks are in the range between $174{,}340 \pm 790$ MeV (for the t-quark) and $1.5 \longleftrightarrow 5$ MeV (for the u-quark); second, the masses of protons and neutrons are 938.272 MeV and 939.565 MeV, respectively; third, the masses of leptons are in the range between 1776.99 MeV (for the τ-lepton) and 0.511 MeV (for the electron); fourth, the masses of the neutrinos are estimated to be in the range between <15.5 MeV (for the τ-neutrino) and <0.0000022 MeV (for the electron neutrino). (The masses of the anti-particles coincide with the ones of the corresponding particles.)

Based on the solutions obtained for two exactly integrable models, we can notice that the effective spinor mass $< M >$ as the function of cosmological time starts from the value m at $t = t_*$, reaches the maximal value (h_0 if $\xi = 0$ and $\frac{1}{2}h_0$ if $\xi = \frac{1}{2}$, and then tends to zero. In fact, we can estimate the parameter h_0 associated with the maximal value of the effective mass as $h_0 > 174{,}340 \pm 790$ MeV for the model with $\xi = 0$ and as $h_0 > 348{,}681 \pm 580$ for the model with $\xi = \frac{1}{2}$. The mass of the electron neutrino, the minimal mass from this catalog, points to the moment of time t_{**} when the self-similar interaction was switched off by the dynamic aether.

5.3. On the Maximal Spinor Particle Number Density

The idea of spontaneous spinorization assumes that during the interval of the cosmological time $t_* < t < t_{**}$, a significant growth of the spinor number density S takes place. This idea is confirmed by the exact solutions (85) (for $\xi = 0$) and (88) (for $\xi = \frac{1}{2}$). Illustrations presented in Figures 2 and 4 visualize the growth of the function $S(t)$. It is important to notice that the maximal value $S_{\max}$ is predetermined by the model guiding parameter h_0. If we suppose that the model with $\xi = 0$ is appropriate, the estimation gives that $S_{\max} \propto S(t_*)4mh_0(t_{\max} - t_+)^2$; for the hypothetical value $h_0 > 174{,}340 \pm 790$ MeV, it is a rather big quantity. If the model with $\xi = \frac{1}{2}$ is more appropriate, the estimations give $S_{\max} \propto S(t_*) \cosh 2h_0(t_{\max} - t_*)$.

5.4. What Is the Energy Source for the Spontaneous Spinorization?

We think that the energy required to increase the number of fermions is drawn from the energy reserve of the gravitational field. The presence of the term $mS + \beta$ in the right-hand side of the Equation (34) hints to us that the energy can be effectively redistributed between the gravitational and spinor fields when the aether opens a window for this process.

5.5. What Do We Think about the Problem of the Lorentz Symmetry Violation in the Context of the Presented Theory?

When the theory of the dynamic aether [23] has been established, the discussions about the so-called Lorentz symmetry violation appeared. There are several levels of meaning in this context. Since we work with the general relativistic approach to the Dirac theory, and thus all the master equations are covariant, we, clearly, do not mean the breaking of invariance with respect to the Lorentz transformations. When we deal with the dynamic aether, we work, in fact, with the Lagrangian, which contains the privileged velocity, the velocity of the aether, thus contradicting with the requirement of the special relativity that all the frames of reference, moving with constant velocities relative to each other, are equivalent. Another item of the mentioned problem is connected with the velocity of photons in the aetheric vacuum: this velocity is not equal now to the constant speed of light in vacuum, it can depend on the photon energy. In other words, the infra-red, optical, and gamma photons can move around the Universe with different velocities.

5.6. Outlook

We hope to apply the presented results to the realistic cosmological model; however, this work is outside the scope of this article. We hope to organize the detailed analysis in the next paper.

Author Contributions: Conceptualization, A.B.; methodology, A.B.; software, A.E.; validation, A.E.; formal analysis, A.E.; investigation, A.B.; resources, A.E.; data curation, A.E.; writing—original draft preparation, A.B.; writing—review and editing, A.B.; visualization, A.E.; supervision, A.B. All authors have read and agreed to the published version of the manuscript.

Data Availability Statement: Data are contained within the article.

Conflicts of Interest: The authors declare no conflict of interest.

References

1. Damour, T.; Esposito-Far'ese, G. Tensor-scalar gravity and binary-pulsars experiments. *Phys. Rev. D* **1996**, *54*, 1474. [CrossRef]
2. Salgado, M.; Sudarsky, D.; Nucamendi, U. On spontaneous scalarization. *Phys. Rev. D* **1998**, *58*, 124003. [CrossRef]
3. Chen, P.; Suyama, T.; Yokoyama, J. Spontaneous scalarization: Asymmetron as dark matter. *Phys. Rev. D* **2015**, *92*, 124016. [CrossRef]
4. Ramazanoglu, F.M.; Pretorius, F. Spontaneous scalarization with massive fields. *Phys. Rev. D* **2016**, *93*, 064005. [CrossRef]
5. Ikeda, T.; Nakamura, T.; Minamitsuji, M. Spontaneous scalarization of charged black holes in the scalar-vector-tensor theory. *Phys. Rev. D* **2019**, *100*, 104014. [CrossRef]
6. Ventagli, G.; Lehebel. A.; Sotiriou, T.P. The onset of spontaneous scalarization in generalised scalar-tensor theories. *Phys. Rev. D* **2020**, *102*, 024050. [CrossRef]
7. Brihaye, Y.; Capobianco, R.; Hartmann, B. Spontaneous scalarization of self-gravitating magnetic fields. *Phys. Rev. D* **2021**, *103*, 124020. [CrossRef]
8. Zhao, J.; Freire, P.C.C.; Kramer, M.; Shao, L.; Wex, N. Closing a spontaneous-scalarization window with binary pulsars. *Class. Quantum Grav.* **2022**, *39*, 11LT01. [CrossRef]
9. Wong, L.K.; Herdeiro, C.A.R.; Radu, E. Constraining spontaneous black hole scalarization in scalar-tensor-Gauss-Bonnet theories with current gravitational-wave data. *Phys. Rev. D* **2022**, *106*, 024008. [CrossRef]
10. Lai, M.Y.; Myung, Y.S.; Yue, R.H.; Zou, D.C. Spin-charge induced spontaneous scalarization of Kerr-Newman black holes. *Phys. Rev. D* **2022**, *106*, 8 084043. [CrossRef]
11. Nakarachinda, R.; Panpanich, S.; Tsujikawa, S.; Wongjun, P. Cosmology in theories with spontaneous scalarization of neutron stars. *Phys. Rev. D* **2023**, *107*, 043512. [CrossRef]
12. Zhang, S.J.; Wang, B.; Papantonopoulos, E.; Wang, A. Magnetic-induced spontaneous scalarization in dynamcial Chern-Simons gravity. *Eur. Phys. J. C* **2023**, *83*, 97. [CrossRef]
13. Annulli, L.; Herdeiro, C.A.R. Non-linear tides and Gauss-Bonnet scalarization. *Phys. Lett. B* **2023**, *845*, 138137. [CrossRef]
14. Ramazanoglu, F.M. Spontaneous growth of vector fields in gravity. *Phys. Rev. D* **2017**, *96*, 064009. [CrossRef]

15. Annulli, L.; Cardoso, V.; Gualtieri, L. Electromagnetism and hidden vector fields in modified gravity theories: Spontaneous and induced vectorization. *Phys. Rev. D* **2019**, *99*, 044038. [CrossRef]
16. Minamitsuji, M. Spontaneous vectorization in the presence of vector field coupling to matter. *Phys. Rev. D* **2020**, *101*, 104044. [CrossRef]
17. Ramazanoglu, F.M. Spontaneous tensorization from curvature coupling and beyond. *Phys. Rev. D* **2019**, *99*, 084015. [CrossRef]
18. Ramazanoglu, F.M. Spontaneous growth of spinor fields in gravity. *Phys. Rev. D* **2018**, *98*, 044011. [CrossRef]
19. Minamitsuji, M. Stealth spontaneous spinorization of relativistic stars. *Phys. Rev. D* **2020**, *102*, 044048. [CrossRef]
20. Balakin, A.B.; Kiselev, G.B. Spontaneous color polarization as a modus originis of the dynamic aether. *Universe* **2020**, *6*, 95. [CrossRef]
21. Balakin, A.B.; Kiselev, G.B. Einstein-Yang-Mills-aether theory with nonlinear axion field: Decay of color aether and the axionic dark matter production. *Symmetry* **2022**, *14*, 1621. [CrossRef]
22. Ramazanoglu, F.M. Spontaneous growth of gauge fields in gravity through the Higgs mechanism. *Phys. Rev. D* **2018**, *98*, 044013. [CrossRef]
23. Jacobson, T.; Mattingly, D. Gravity with a dynamical preferred frame. *Phys. Rev. D* **2001**, *64*, 024028. [CrossRef]
24. Jacobson, T.; Mattingly, D. Einstein-aether waves. *Phys. Rev. D* **2004**, *70*, 024003. [CrossRef]
25. Heinicke, C.; Baekler, P.; Hehl, F.W. Einstein-aether theory, violation of Lorentz invariance, and metric-affine gravity. *Phys. Rev. D* **2005**, *72*, 025012. [CrossRef]
26. Jacobson, T. Einstein-aether gravity: A status report. In Proceedings of the Workshop on from Quantum to Emergent Gravity: Theory and Phenomenology (QG-Ph), Trieste, Italy, 11–15 June 2007; p. 20.
27. Eling, C.; Jacobson, T.; Miller, M.C. Neutron stars in Einstein-aether theory. *Phys. Rev. D* **2007**, *76*, 042003. [CrossRef]
28. Barausse, E.; Jacobson, T.; Sotiriou, T.P. Black holes in Einstein-aether and Horava-Lifshitz gravity. *Phys. Rev. D* **2011**, *83*, 124043. [CrossRef]
29. Nojiri, S.; Odintsov, S.D. Unified cosmic history in modified gravity: From F(R) theory to Lorentz non-invariant models. *Phys. Rept.* **2011**, *505*, 59. [CrossRef]
30. Nojiri, S.; Odintsov S.D.; Oikonomou, V.K. Modified gravity theories on a nutshell: Inflation, bounce and late-time evolution. *Phys. Rept.* **2017**, *692*, 1. [CrossRef]
31. Will, C.M.; Nordtvedt, K. Conservation laws and preferred frames in relativistic gravity. I. Preferred-frame theories and an extended PPN formalism. *Astrophys. J.* **1972**, *177*, 757. [CrossRef]
32. Nordtvedt, K.; Will, C.M. Conservation laws and preferred frames in relativistic gravity. II. Experimental evidence to rule out preferred-frame theories of gravity. *Astrophys. J.* **1972**, *177*, 775–792. [CrossRef]
33. Liberati, S. Lorentz breaking effective field theory and observational tests. *Lect. Notes Phys.* **2013**, *870*, 297.
34. Kostelecky, A.; Mewes, M. Electrodynamics with Lorentz-violating operators of arbitrary dimension. *Phys. Rev. D* **2009**, *80*, 015020. [CrossRef]
35. Fock, V.; Iwanenko, D. Geometrie quantique lineaire et deplacement parallele. *Compt. Rend. Acad. Sci.* **1929**, *188*, 1470.
36. Volkov, M.S.; Gal'tsov, D.V. Gravitating non-Abelian solitons and black holes with Yang-Mills fields. *Phys. Rept.* **1999**, *319*, 1. [CrossRef]
37. Balakin, A.B. Extended Einstein-Maxwell model. *Gravit. Cosmol.* **2007**, *13*, 163.
38. Abbott, B.P. et.al. [LIGO Scientific Collaboration; Virgo Collaboration; Fermi Gamma-Ray Burst Monitor; INTEGRAL]. Gravitational waves and gamma-rays from a binary neutron star merger: GW170817 and GRB 170817A. *APJ Lett.* **2017**, *848*, L13. [CrossRef]
39. Elliott, J.W.; Moore, G.D.; Stoica, H. Constraining the new aether: Gravitational Cherenkov radiation. *J. High Energy Phys.* **2005**, *0508*, 066. [CrossRef]
40. Kostelecky, A.; Tasson, J.D. Constraints on Lorentz violation from gravitational Cherenkov radiation. *Phys. Lett. B* **2015** *749*, 551. [CrossRef]
41. Oost, J.; Mukohyama, S.; Wang, A. Constraints on Einstein-aether theory after GW170817. *Phys. Rev. D* **2018**, *97*, 124023. [CrossRef]
42. Trinh, D.; Pace, F.; Battye, R.A.; Bolliet, B. Cosmologically viable generalized Einstein-Aether theories. *Phys. Rev. D* **2019**, *99*, 043515.
43. Balakin, A.B.; Shakirzyanov, A.F. Axionic extension of the Einstein-aether theory: How does dynamic aether regulate the state of axionic dark matter? *Phys. Dark Univ.* **2019**, *24*, 100283. [CrossRef]
44. Saha, B.; Shikin, G.N. Nonlinear spinor field in Bianchi type-I universe filled with perfect fluid: Exact self-consistent solutions. *J. Math. Phys.* **1997**, *38*, 5305. [CrossRef]
45. Saha, B. Spinor field in Bianchi type-I universe: regular solutions. *Phys. Rev. D* **2001**, *64*, 123501. [CrossRef]
46. Saha, B. Nonlinear spinor field in cosmology. *Phys. Rev. D* **2004**, *69*, 124006. [CrossRef]
47. Bronnikov, K.A.; Rybakov, Yu, P.; Saha, B. Spinor fields in spherical symmetry. Einstein-Dirac and other space-times. *Eur. Phys. J. Plus* **2020**, *135*, 124. [CrossRef]

48. Saha, B.; Boyadjiev, T. Bianchi type I cosmology with scalar and spinor fields. *Phys. Rev. D* **2004**, *69*, 124010. [CrossRef]
49. Balakin, A.B.; Efremova, A.O. Interaction of the axionic dark matter, dynamic aether, spinor and gravity fields as an origin of oscillations of the fermion effective mass. *Eur. Phys. J. C* **2021**, *81*, 674. [CrossRef]